# Scattering of a matter-wave single soliton and a two-soliton molecule by an attractive potential

S. M. Al-Marzoug,[1] S. M. Al-Amoudi,[1] U. Al Khawaja,[2] H. Bahlouli,[1,3] and B. B. Baizakov[4]
[1]*Department of Physics, King Fahd University of Petroleum and Minerals, Dhahran 31261, Saudi Arabia*
[2]*Physics Department, United Arab Emirates University, P.O. Box 17551, Al-Ain, United Arab Emirates*
[3]*Saudi Center for Theoretical Physics, Dhahran 31261, Saudi Arabia*
[4]*Physical-Technical Institute, Uzbek Academy of Sciences, 100084, Tashkent, Uzbekistan*
(Received 30 June 2010; revised manuscript received 28 October 2010; published 24 February 2011)

Scattering of a matter-wave single soliton and two-soliton molecule incident on the modified Pöschl-Teller potential well has been studied by means of a collective coordinate approach and numerical simulations of the Gross-Pitaevskii equation. Despite the attractive nature of the potential we observe total reflection of solitons in particular ranges of parameters, which is the signature of quantum behavior displayed by the matter-wave soliton. For other particular sets of parameters unscathed transmission of solitons and molecules through the potential well has been identified. A specific feature of this process is that the soliton passing through the potential well overtakes the freely propagating counterpart; i.e., its mean position appears to have been advanced in time. An array of such potentials makes the "time advance" effect even more pronounced, so that scattered solitons move well ahead of nonscattered ones, fully preserving their initial shape and velocity. A possible application of the obtained results is pointed out.

DOI: 10.1103/PhysRevE.83.026603 PACS number(s): 05.45.Yv, 03.75.Lm, 03.65.Xp

## I. INTRODUCTION

Signatures of quantum behavior in the dynamics of macroscopic objects always attract vivid interest. One of the recent observations in this direction has been the quantum reflection of matter-wave solitons from attractive potentials [1,2] and negative potential steps [3]. The term *quantum* refers to the fact that reflection occurs without reaching a classical turning point, and to its relevance to the wave nature of the soliton. An intriguing point is that quantum reflection is manifested by a matter-wave soliton, which represents a self-trapped state of a large number ($N \sim 10^3$) of ultracold atoms spatially extended to a macroscopic size ($d \sim 1$–$10\ \mu$m), and therefore in most circumstances considered to be a classical object. Indeed, the Gross-Pitaevskii equation (GPE), describing the condensate dynamics in the mean field regime, contains nonlinearity which gives rise to the existence of solitons, exhibiting particle-like properties in many respects [4]. The combination of the wave and particle properties of matter-wave solitons makes them unique objects for exploring the role of nonlinearity in macroscopic (many body) quantum transport (reflection, transmission, and tunneling) phenomena [5,6].

Certain potentials for the one-dimensional Schrödinger equation possess a remarkable property that any incident wave packet with arbitrary momentum traverses the scattering region with probability one. These so-called *reflectionless* potentials (RLP) have been extensively investigated, most notably in the context of soliton bearing wave equations [7]. When applied to a Gaussian wave packet instead of a plane wave it was noticed that traversing the RLP gives rise to a focusing (narrowing in width and rising in height) of the incident wave packet and advancement of its mean position in time as compared to the freely evolved wave packet in absence of any potential [8].

Reflection and transmission of matter-wave packets through RLPs in the presence of nonlinearity, when the wave packet's evolution is governed by the GPE instead of the linear Schrödinger equation, represents an interesting and less explored subject. In this paper we investigate these phenomena, both analytically and numerically, by setting in motion a single soliton and two-soliton molecule toward the modified Pöschl-Teller potential, which is the most prominent example of RLPs [9]. The analytical part is based on the collective coordinate approach (also known as the variational approximation), which was summarized in a recent review [10]. This approach is well suited for the investigation of soliton interactions with localized impurities. In particular, the possibility of total reflection and trapping of the soliton by an attractive impurity, when the incident soliton is sufficiently slow, was demonstrated in [11] taking the sine-Gordon and $\phi^4$ models as examples. The birth of soliton internal modes resulting from the interaction with an impurity and the associated resonant phenomena were studied in [12]. Scattering and trapping of solitons by a rectangular potential well in the nonlinear Schrödinger equation was reported in [13] using the collective coordinate approach.

Our main objective in this work is to identify similarities and differences between the quantum reflection of a single soliton and two-soliton molecule, as well as to find conditions when the reflected and transmitted soliton molecule retains its integrity. In addition, we explore the above mentioned "time advance" (TA) phenomenon [8] for matter-wave solitons and molecules traversing the RLP.

Regarding the soliton molecule in the present setting, it should be stressed that it is different from the one found in dispersion-managed optical fiber systems [14]. Some properties of soliton molecules in the present configuration have been analyzed recently in [15]. In particular, the role of the relative phase between solitons in the formation of a soliton molecule and the stability of a soliton molecule subject to different perturbations, such as reflection from potential barriers and surfaces and collision with other solitons, were investigated by analytical and numerical means. However, the problem of quantum reflection of a soliton molecule from attractive potentials, as well as the TA phenomenon in the context of

 

matter-wave solitons and molecules traversing RLPs, to the best of our knowledge, has not been addressed so far.

The paper is organized as follows. In Sec. II we introduce the model, governing equations, and statement of the problem. Section III is devoted to collective coordinate analysis of the model, while in Sec. IV we perform numerical simulations of the dynamics of a matter-wave single soliton and two-soliton molecule interacting with the RLP. In Sec. V we summarize our findings.

## II. FORMULATION OF THE PROBLEM

The model is based on the Gross-Pitaevskii equation, which governs the mean-field dynamics of the condensate:

$$i\hbar\frac{\partial\Psi}{\partial t}=\left[-\frac{\hbar^2}{2m}\nabla^2+\frac{1}{2}m\omega_\perp^2 r^2+V(x)+\frac{4\pi\hbar^2 a_s}{m}|\Psi|^2\right]\Psi, \tag{1}$$

where $\Psi$ is the macroscopic wave function of the condensate, normalized to the number of atoms $N=\int_{-\infty}^{\infty}|\Psi|^2 d\mathbf{r}$ with mass $m$ and characterized by the $s$-wave scattering length $a_s$. Both signs of this parameter are physically relevant: the positive sign ($a_s>0$) corresponds to repulsive interatomic interactions in the condensate, while the negative sign ($a_s<0$) implies attractive interactions. To avoid collapse instability inherent in 3D BEC with focusing nonlinearity, the initial $s$-wave scattering length should be positive, but tuned to a negative value, employing the Feshbach resonance technique [16], at the stage of generation of solitons [17]. Strong confinement in the radial direction ($r^2=y^2+z^2$) creates a quasi-1D waveguide for the condensate with trapping frequency $\omega_\perp$. The condensate acquires a cigar shape when the longitudinal size of the condensate is much greater than both the healing length $\xi=(8\pi n_0 a_s)^{-1/2}$, where $n_0$ is the peak density of BEC, and the radial oscillator length. In addition, the chemical potential has to be much less than the radial harmonic oscillator ground state energy to suppress radial excitations of the condensate. When these conditions are met, the condensate displays a quasi-1D behavior. This setting, however, assumes some initial trapping potential in the axial direction as well. The scattering potential $V(x)$ can be created by a laser beam with the frequency red detuned from atomic transitions, so that the resulting force on condensate atoms points in the direction of increasing field intensity, as in optical traps.

As mentioned above, when the radial confinement is strong enough, the transverse dynamics of the condensate is suppressed, which means that one can factorize the wave function as follows:

$$\Psi(r,x,t)=\psi(x,t)\,\phi(r)\exp(-i\omega_\perp t), \tag{2}$$

where

$$\phi(r)=\frac{1}{\pi^{1/2}a_\perp}\exp\left(-\frac{r^2}{2a_\perp^2}\right)$$

is the ground state wave function of the radial harmonic trap, with $a_\perp=\sqrt{\hbar/m\omega_\perp}$ being its characteristic length. The substitution of Eq. (2) into Eq. (1) and integration over the transverse variable $r$ yields the 1D GPE for the longitudinal wave function $\psi(x,t)$:

$$i\hbar\psi_t=-\frac{\hbar^2}{2m}\psi_{xx}+V(x)\psi+2\hbar\omega_\perp a_s|\psi|^2\psi, \tag{3}$$

where the indices in $\psi(x,t)$ denote the corresponding derivatives. Finally, by introducing dimensionless variables $t\to\omega_\perp t, x\to x/a_\perp, g=-2a_s/a_\perp, V(x)\to V(x)/\hbar\omega_\perp$, and $\psi\to a_\perp^{1/2}\psi$, we obtain the main equation of our model:

$$i\psi_t+\tfrac{1}{2}\psi_{xx}-V(x)\psi+g\,|\psi|^2\psi=0. \tag{4}$$

We consider the BEC wave packet with attractive interaction between atoms ($a_s<0$, therefore $g>0$) confined in a quasi-1D atomic waveguide, so that the system supports bright matter-wave solitons [18].

In the following, we study the scattering of a single soliton and two-soliton molecule by the modified Pöschl-Teller potential well [9]

$$V(x)=-\frac{V_0}{\cosh^2(\alpha x)} \tag{5}$$

characterized by the strength $V_0>0$ and inverse width $\alpha$. Thanks to its remarkable property of transmitting linear waves of arbitrary momentum, at some values of $V_0$ and $\alpha$, without attenuation, this potential is of particular interest also to nonlinear wave scattering. In the presence of nonlinearity, the transmission characteristics of potential wells appear to be strongly modified. In particular, resonant transmission peaks predicted by linear theory change to transmission windows, but their positions remain the same [2]. Besides, for ordinary potentials like the square well, the transmission of the wave packet is not perfect even at resonant conditions due to inevitably present reflected waves [2]. Interference with these reflected waves is detrimental to the integrity of the soliton molecule traversing the potential well, which is the reason for giving preference to RLPs in our studies.

A sketch of the two-soliton molecule being scattered by a RLP is shown in Fig. 1. The initial position of the molecule $x=0$ is far from the potential well situated at $x_p$, so that there is no interaction between them at $t=0$. At time $t_c\sim x_p/v$ the molecule, set in motion with the velocity $v$, interacts with the potential well and partially reflects ($R$), transmits ($T$),

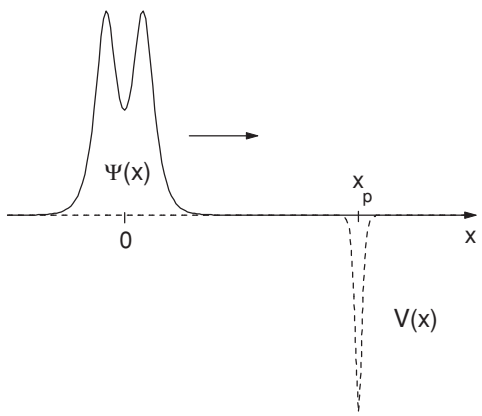


FIG. 1. Sketch of the two-soliton molecule being scattered by the attractive potential well.

or gets trapped ($L$) by it. The relative values of these three quantities strongly depend on the molecule's velocity and strength of the potential well, reaching at some particular combinations of parameters ($v$ vs $V_0$) the total reflection ($R \simeq 1$), full transmission ($T \simeq 1$), or total trapping ($L \simeq 1$), while the conservation law $R + T + L = 1$ is ensured. These parameters are calculated at time $t = 2t_c$, i.e., well after the scattering from the potential well, according to the relations

$$R = \frac{1}{\mathcal{N}} \int_{-\infty}^{-h} |\psi(x)|^2 dx, \quad T = \frac{1}{\mathcal{N}} \int_{h}^{\infty} |\psi(x)|^2 dx, \quad L = \frac{1}{\mathcal{N}} \int_{-h}^{h} |\psi(x)|^2 dx, \tag{6}$$

where $h$ denotes position on the $x$ axis at which the effect of the potential vanishes $V(h) \sim 0$, and $\mathcal{N} = \int_{-\infty}^{\infty} |\psi(x)|^2 dx$ is the 1D norm (number of atoms) of the soliton or molecule.

To study the scattering of a soliton molecule by RLP we employ the well-known bound state of two bright solitons, whose properties have been explored in the context of optical soliton based communications systems (for a review see [19] and references therein). Several authors have investigated the dynamics of two or more matter-wave solitons confined to harmonic traps [20]. Our model distinguishes itself from other relevant works by considering the situation when the confining potential for the matter-wave soliton molecule is absent, while the potential participating in the scattering process has an attractive nature to ensure nonclassical reflection [21].

As an initial condition for Eq. (4) with $g = 1$ we employ a bound state of two fundamental solitons separated by a distance $2x_0$, and zero phase difference:

$$\psi(x,0) = \mathrm{sech}(x - x_0) + \mathrm{sech}(x + x_0). \tag{7}$$

In the absence of external potential [$V(x) = 0$] and a not too large initial separation, the two solitons in this configuration attract each other to form a molecule and oscillate with a period given by [19]

$$t_p = \frac{\pi \sinh(2x_0)\cosh(x_0)}{2x_0 + \sinh(2x_0)}. \tag{8}$$

The interaction dynamics of two solitons, including the configuration given by Eq. (7), is well studied in the context of optical soliton propagation in fibers [19,22–24]. Although the wave profile (7) is not an exact two-soliton bound state of the original Eq. (4) without external potential, it was shown numerically to be very close to it for arbitrary separation. In particular, the maximum error incurred by the approximation does not exceed 2% and less than 0.1% of the total energy of the configuration sheds off during the evolution as a nonsoliton part [19]. This means that the bound state of two solitons, represented by Eq. (7), can be considered a long-lived soliton molecule to a very good approximation. As will be shown in subsequent parts of the paper, solitons in the molecule remain bounded for a long time after reflections from and transmissions through potential wells.

## III. COLLECTIVE COORDINATE APPROACH

The collective coordinate approach represents one of the important theoretical tools for the analysis of nonintegrable soliton bearing equations. Below we consider the transmission of a single soliton through a potential well and the associated excitation of its internal modes using the collective coordinate approach. The excited internal mode manifests itself as a small amplitude oscillation of the soliton's shape, which can be described in terms of a chirp parameter. The excitations of internal modes of the soliton molecule can be qualitatively analyzed using the same argument.

The Lagrangian generating the dimensionless GPE (4) is

$$\mathcal{L} = \frac{i}{2}(\psi\psi_t^* - \psi^*\psi_t) + \frac{1}{2}|\psi_x|^2 - V(x)|\psi|^2 - \frac{1}{2}|\psi|^4. \tag{9}$$

Since the calculation of the effective Lagrangian $L = \int_{-\infty}^{\infty} \mathcal{L} dx$ with the original potential (5) is complicated, for a qualitative analysis we replace it by a delta function, approximated by the following expression [25]:

$$\delta(x,\alpha) = \frac{\alpha}{\pi(\alpha^2 x^2 + 1)}, \quad \text{at} \quad \alpha \to \infty. \tag{10}$$

Then, taking into account the relation $\lim_{\alpha\to\infty} \cosh^2(\alpha x) = \alpha^2 x^2 + 1$, we can replace the narrow and deep Pöschl-Teller potential (5) by a delta function:

$$V(x) \simeq -U_0\delta(x), \quad \text{where} \quad U_0 = \frac{\pi V_0}{\alpha}. \tag{11}$$

The success of the collective coordinate approach strongly depends on the right choice of the trial function. In the problem at hand we have a freely propagating soliton when it is sufficiently far from the scattering potential well. Therefore, an appropriate trial function would be the exact soliton solution of Eq. (4) for $V(x) = 0$:

$$\psi(x,t) = A\ \mathrm{sech}\left(\frac{x-\xi}{a}\right) e^{ib(x-\xi)^2 + iv(x-\xi) + i\phi}, \tag{12}$$

where $A, a, \xi, b, v, \phi$ are time dependent collective coordinates, standing for the amplitude, width, center-of-mass position, chirp parameter, velocity, and phase of the soliton, respectively. On the other hand, when the soliton enters the region of the potential well its quantum bound states start to build up. Numerical simulations of the GPE (4) with the original potential (5) show that all bound states are populated simultaneously. Therefore the collective coordinate equations with the general trial function, which includes all bound states of the potential, would be rather complicated.

Below we demonstrate that the main phenomena studied in the present work, namely the so called time advance effect and excitation of internal modes of the soliton traversing the potential well, are well described through the simplified trial function (12) and potential (11). Evaluation of the effective Lagrangian using the above trial function is straightforward

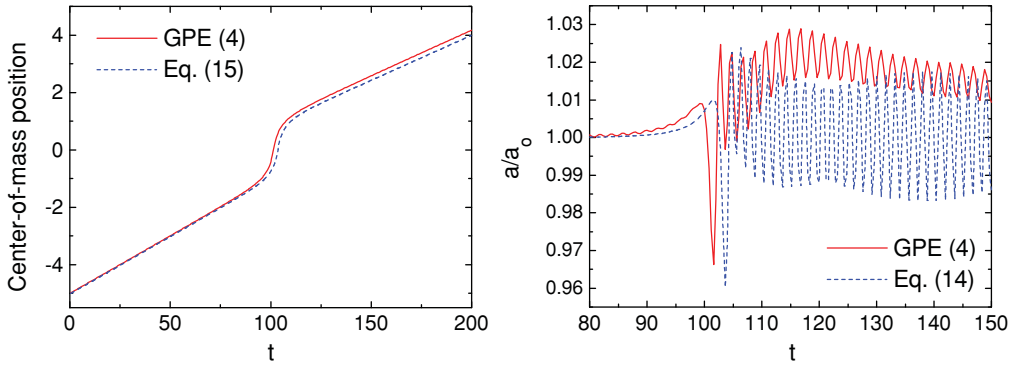


FIG. 2. (Color online) Left panel: Center-of-mass position of a soliton passing through the delta-potential well as obtained from direct simulation of the GPE (4), and as predicted by the collective coordinate equations (15). Right panel: Oscillations of the soliton's width due to excitation of internal modes, as predicted by the GPE (4) and collective coordinate Eq. (14).

and leads to

$$L = N\left[\frac{\pi^2}{12}a^2 b_t - \frac{\xi_t^2}{2} + \phi_t + \frac{\pi^2}{6}a^2 b^2 + \frac{1}{6a^2} - \frac{U_0}{2a}\,\mathrm{sech}^2\left(\frac{\xi}{a}\right) - \frac{N}{6a}\right], \tag{13}$$

where the norm $N = \int_{-\infty}^{\infty}|\psi|^2 dx = 2A^2 a$ is a conserved quantity. Dynamical equations are obtained from the Euler-Lagrange equations $(d/dt)\partial L/\partial\dot{q}_i - \partial L/\partial q_i = 0$, with $q_i$ being the above mentioned collective coordinates. Note that the equation for the phase $\phi$ is decoupled from other equations giving the conservation of the norm $dN/dt = 0$. Eventually we get the coupled equations for the soliton's width and center-of-mass position:

$$a_{tt} = \frac{4}{\pi^2 a^3} - \frac{2N}{\pi^2 a^2} - \frac{6U_0}{\pi^2 a^2}\mathrm{sech}^2\left(\frac{\xi}{a}\right)\left[1 - \frac{2\xi}{a}\mathrm{th}\left(\frac{\xi}{a}\right)\right], \tag{14}$$

$$\xi_{tt} = -\frac{U_0}{a^2}\mathrm{sech}^2\left(\frac{\xi}{a}\right)\mathrm{th}\left(\frac{\xi}{a}\right). \tag{15}$$

When the soliton's internal modes are excited due to some perturbation, e.g., interaction with the potential well, its shape performs small amplitude vibrations around the stationary state. In particular, after traversing the potential well the soliton can exhibit long-lived oscillations of its width described by Eq. (14). The frequency of internal modes can be estimated from the following arguments. When the soliton leaves the interaction region with the potential well ($\xi \gg a$), its center-of-mass dynamics becomes decoupled from the dynamics of its width. Then we obtain the freely propagating soliton $\xi_{tt} = 0$, whose width oscillates according to the following nonlinear equation:

$$a_{tt} = -\frac{\partial W(a)}{\partial a}, \quad \text{with} \quad W(a) = \frac{2}{\pi^2 a^2} - \frac{2N}{\pi^2 a}. \tag{16}$$

The stationary width of the soliton is found from the fixed point of this equation $a_0 = 2/N$. Linearizing Eq. (14) around the stationary state $a(t) = a_0 + a_1(t)$ with $a_1 \ll a_0$, one obtains the corresponding equation and the frequency of small amplitude oscillations of the soliton's width, i.e., the frequency of its internal modes:

$$a_{1tt} + \omega_0^2 a_1 = 0, \quad \omega_0 = N^2/(2\pi). \tag{17}$$

In Fig. 2 the prediction of the collective coordinate approach is compared with direct numerical simulation of the governing GPE (4). The delta function potential is modeled by expression (10) with $\alpha = 100$. The soliton with amplitude $A = 2.5$ and width $a = 0.4$ is set in motion with a velocity $v = 0.04$ from the initial position $x = -5$ toward the delta potential well of strength $U_0 = 0.05$, located at the origin $x = 0$. As can be seen from this figure, the soliton moves with acceleration while traversing the interaction region with the potential, but restores its initial velocity afterward. As a result its center-of-mass coordinate appears to be advanced compared to a freely propagating soliton. This interesting feature is observed also with the original reflectionless potential (5) described in the next section. Besides, interaction with the potential well gives rise to excitation of internal modes of the soliton, as illustrated in the right panel of Fig. 2. The frequency of the soliton's internal mode calculated from Eq. (17) for the accepted parameters is $\omega_0 = 3.9$, while the result from the numerical solution of the GPE (4) is $\omega_0 = 3.1$. Despite the relative discrepancy $\sim$20%, which can be attributed to the highly nonlinear character of the oscillations, the collective coordinate approach provides a satisfactory description of single-soliton scattering by an attractive potential.

The collective coordinate approach for the dynamics of a two-soliton bound state given by Eq. (7), in the absence of external potential, was developed in [23]. The governing system consists of eight coupled equations. Extension of this model to the case of independent amplitude and width of the soliton, and also inclusion of the chirp parameter, would increase the number of equations and complicate the analysis. Below we consider the problem of internal modes of the soliton molecule qualitatively.

According to the collective coordinate approach, the time-dependent width of the soliton is linked to the chirp parameter in Eqs. (12) and (13) as $b = (d\ln a/dt)/2$. Therefore the soliton whose internal modes are excited due to the interaction with the potential well can be regarded as a chirped soliton.

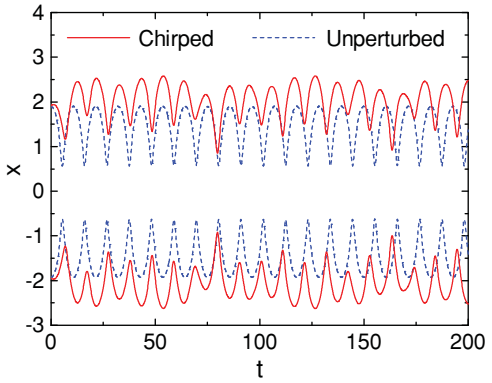


FIG. 3. (Color online) Evolution of the center-of-mass positions of individual solitons of the molecule (7), whose solitons are equally chirped with $b = 0.15$. Quasiperiodic dynamics due to the excitation of internal modes of the soliton molecule is clearly observed. For comparison the dynamics of an unperturbed soliton molecule is also shown. Note that when two solitons coalesce center-of-mass positions of individual solitons cannot be defined.

This argument allows us to make a qualitative analysis of the dynamics of a two-soliton molecule induced by its interaction with the scattering potential. Namely, we assume that both solitons of the molecule acquire an equal chirp due to the interaction. Figure 3 illustrates the excitation of the internal mode of a two-soliton molecule due to such a process.

## IV. NUMERICAL SIMULATIONS

Numerical simulations of the GPE (4) with a single soliton and two-soliton initial conditions (7) have been performed using the split-step fast Fourier transform method, which proved to be efficient in solving similar problems in nonlinear fiber optics [26]. The integration domain has been selected wide enough (20–40 times the molecule's bond length) to prevent boundary effects. In addition, a small number of linear waves emitted by the soliton molecule due to its interaction with the potential are absorbed at domain boundaries using the technique described in [27]. In this way the infinite boundary condition for Eq. (4) has been emulated. Most of the numerical simulations are performed using the time step $\delta t = 0.001$ and 1024 Fourier modes. Occasionally we have double checked the results by increasing the number of Fourier modes to 2048 in order to verify the absence of aliasing effects [28] and to ensure the stability of the program.

### A. Results for single-soliton scattering

Detailed analysis of the matter-wave single-soliton reflection and transmission by potential wells was reported in [1,2]. Below we shall be concerned with the novel aspect of the soliton scattering by attractive potentials, namely with the above mentioned TA effect. The phenomenon that the mean position of a linear wave packet incident on a reflectionless potential appears to have been *advanced in time* after the scattering event, compared to the freely propagated counterpart, was first noticed in the transmission of a Gaussian wave packet through such a potential [8]. In the linear case described by the Schrödinger equation, the Gaussian wave packet reassembles after the scattering event, becoming taller and narrower than the nonscattered wave packet. The key difference in the case of nonlinear wave transmission is that the wave packet preserves its initial shape after the scattering event. In Fig. 4 we illustrate the scattering process, where the soliton preserves its initial shape after multiple passages through a chain of successive potential wells. Meanwhile, conditions for the reflectionless transmission are strongly modified for nonlinear wave packets. Namely, while the linear wave of arbitrary momentum, incident on the potential well $V(x) = -\alpha^2\lambda(\lambda - 1)/\cosh^2(\alpha x)$, is fully transmitted at any integer value of $\lambda$ [9], the momentum of the nonlinear wave packet has to exceed some critical value for the full transmission [1].

As can be seen from Fig. 4 the soliton passing through the potential well overtakes the freely propagating counterpart; i.e., its center-of-mass position appears to have been advanced

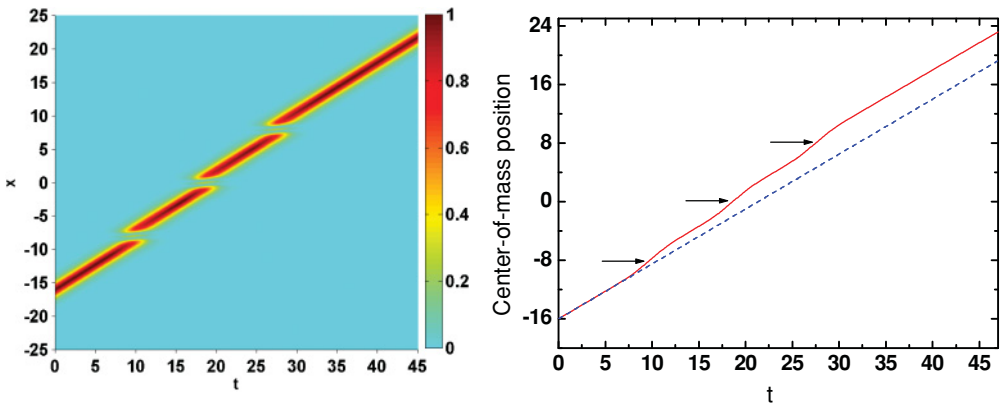


FIG. 4. (Color online) Illustration for the "time advance" effect. Unscathed transmission of a single matter-wave soliton $\psi(x,0) = \mathrm{sech}(x)$ through a chain of three potential wells (5), according to numerical solution of the GPE (4). Soliton's center-of-mass position appears to have been advanced in time after each scattering event. Parameters of the potential (5) positioned at $x = -8$, $x = 0$, and $x = 8$ (shown by arrows) are $V_0 = 12.85$ and $\alpha = 2$. Soliton is set in motion with velocity $v = 0.75$ from initial position $x = -16$. Left panel: Density plot of the soliton passing through the chain of potential wells. Right panel: Evolution of the soliton's center-of-mass coordinate (red solid line) compared with the freely evolved counterpart (blue dashed line), highlighting the TA effect. Scattered soliton moves well ahead of the nonscattered counterpart.

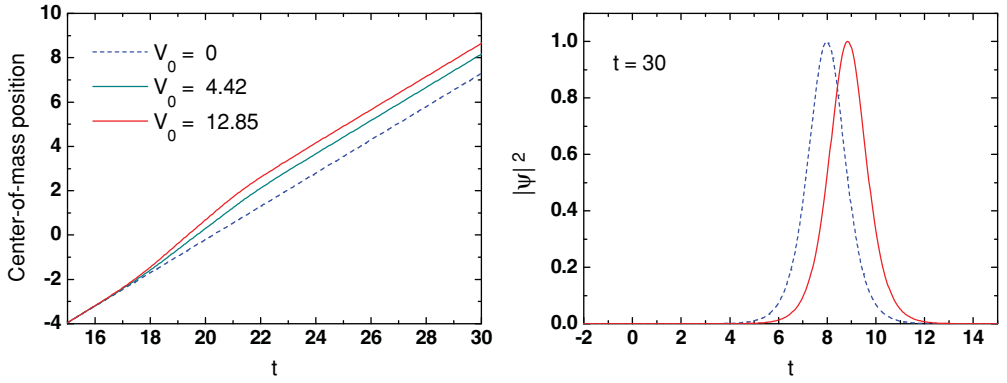


FIG. 5. (Color online) Left panel: Position of a soliton passing through potential wells of different depth as a function of time. TA effect becomes stronger as the depth of the potential well increases. Single soliton is set in motion with a velocity $v = 0.75$ toward the potential well (5) with $\alpha = 2$ and different depths $V_0$. Right panel: Comparison of soliton profiles at $t = 30$. Passage through the RLP leads only to advancement of the soliton's center-of-mass position, but its shape remains intact.

in time. An array of such potentials makes the TA effect even more pronounced, so that the scattered soliton moves well ahead of the nonscattered one, fully preserving its initial shape and velocity. This property can be suggestive for interesting applications of the phenomenon. For instance, to change the interpulse distance in a soliton train propagating along the waveguide it would be enough to make the selected soliton pass through the RLP, temporarily created by a red detuned laser beam. The absence of adverse effects of manipulation like pulse deformation, emission of linear waves, and change of the soliton's velocity are among the main advantages of the proposed scheme based on RLPs.

The mechanism behind the TA effect is that the soliton moves with acceleration under the influence of the attractive potential. When it leaves the zone of the potential, it acquires the same velocity as before the interaction. Indeed, it is evident from the right panel of Fig. 4 that the corresponding (solid and dashed) lines are parallel after the scattering event (see also the left panel of Fig. 2). Deeper potential wells cause stronger shift of the traversing soliton's center-of-mass position, as shown in Fig. 5.

The TA can be estimated from energy conservation arguments [8]. Suppose that the soliton is represented by a particle with mass $m$ and initial velocity $v_0$. Far from the potential well it possesses only the kinetic energy $mv_0^2/2$. When entering the region of action of the potential well it acquires also a potential energy $V(x)$ and may change its velocity under the action of the potential. Then the energy conservation condition has the form

$$\frac{mv_0^2}{2} = \frac{mv^2(x)}{2} + V(x). \tag{18}$$

This equation can be arranged to give

$$dt = \frac{dx}{\sqrt{v_0^2 - \frac{2V(x)}{m}}}. \tag{19}$$

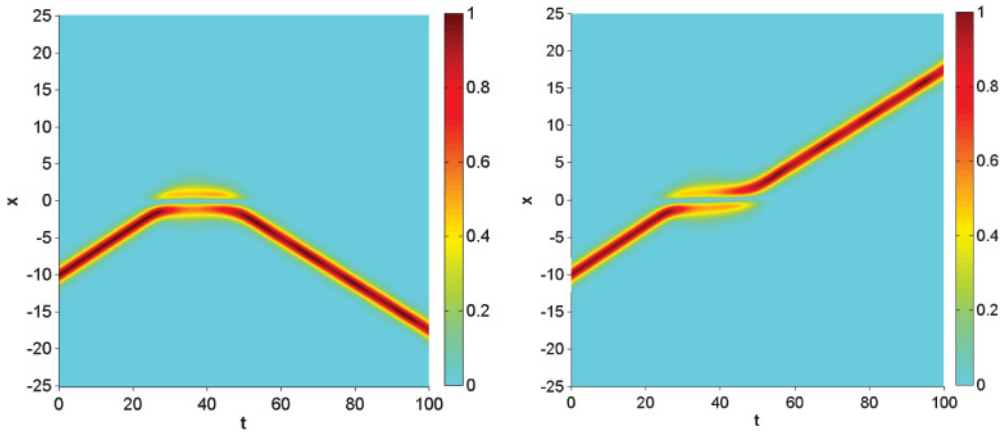


FIG. 6. (Color online) Illustration for the "time delay" effect. The intrinsic mode of the RLP (5) grows by resonantly extracting energy from the soliton. When it becomes large enough, the two modes exchange energy, eventually pulling the soliton out of the potential well, either as reflection (left panel), or transmission (right panel). The mean position of the soliton, traversing the RLP, appears to have been delayed in time, compared to the nonscattered soliton. Parameters: $V_0 = 4$, $\alpha = 2$, $v = 0.325$ (left panel), $v = 0.330$ (right panel). Initial position of the soliton is at $x_p = -10$.

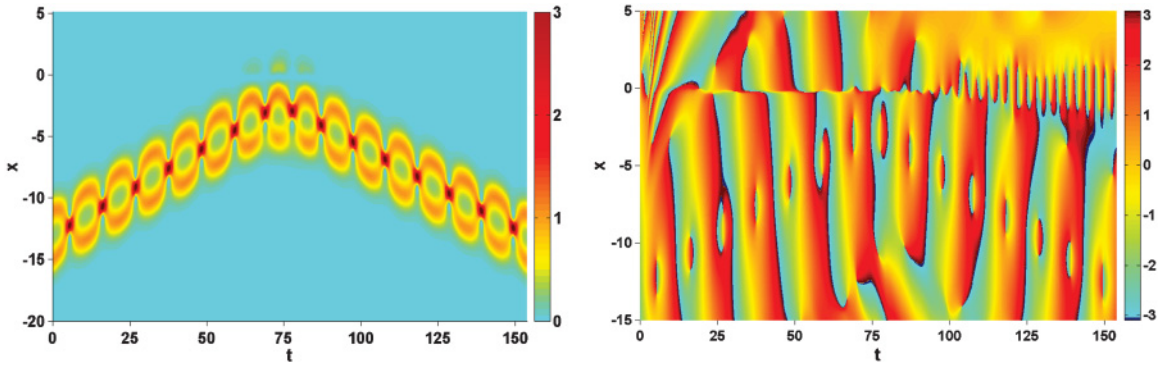


FIG. 7. (Color online) Quantum reflection of the soliton molecule incident on the attractive potential (5) with parameters $V_0 = 4$, $\alpha = 2$, positioned at $x = 0$. Left panel: Totally nondestructive reflection of a soliton molecule with velocity $v = 0.144$ and initial position of its center of mass $x_p = -13$. Right panel: Evolution of the phase showing that coalescing and separating solitons in the molecule preserve zero phase difference (the same color). Meanwhile the intrinsic mode of the potential well, formed by the approaching soliton, has opposite sign, ensuring the repulsion between the intrinsic mode and soliton molecule.

From the last equation we have the estimate for the TA due to passage through one potential well:

$$\tau = \int_{-\infty}^{\infty} \left( \frac{1}{v_0} - \frac{1}{\sqrt{v_0^2 - 2V(x)/m}} \right) dx, \qquad (20)$$

where we have used the fact that at $t = 0$ the soliton is far away from the potential well [$V(x) \to 0$] and has the velocity $v_0$. Now we estimate the last integral for the potential (5). Using the property $V(-x) = V(x)$, we can write

$$\tau = \frac{2}{\alpha v_0} \int_0^{\infty} \left[ 1 - \frac{1}{\sqrt{1 + \frac{2V_0}{m v_0^2} \mathrm{sech}^2(x)}} \right] dx. \qquad (21)$$

By introducing the new variable $y = \mathrm{sech}(x)$ and a constant $c = \frac{2V_0}{m v_0^2}$, we can rewrite the last equation in the form

$$\tau = \frac{2}{\alpha v_0} \int_0^1 \frac{\sqrt{1 + cy^2} - 1}{y\sqrt{1 - y^2}\sqrt{1 + cy^2}} dy = \frac{\ln(1 + c)}{\alpha v_0}. \qquad (22)$$

Equation (4) can be considered the analog of the original 1D GPE (3) for $\hbar = m = 1$, but with time and strength of the potential measured in units of $\omega_\perp$. Therefore, for parameter values $\alpha = 2$, $V_0 = 12.85$, and $v_0 = 0.75$ corresponding to Fig. 4, we have

$$\tau = \frac{1}{\alpha v_0} \ln\left( 1 + \frac{2V_0}{v_0^2} \right) \simeq 2.56. \qquad (23)$$

For a soliton which has passed three potential wells this gives a shift $\delta x = 3v_0\tau \simeq 5.7$ of center-of-mass position with respect to the freely propagated counterpart. The last estimate, although it exceeds the numerical result of Fig. 4, namely $\delta x \simeq 4$, seems to be reasonable, given the fact that we have not taken into account in Eq. (18) the energy due to the nonlinear term. Deformations of the soliton passing through the potential well may also contribute to total energy balance (18); however, this issue is beyond the scope of the present work.

While discussing the "time advance" effect, it is pertinent to mention also the existence of a "time delay" (TD) effect in the scattering of solitons by RLPs. However, its mechanism is different from that of the TA effect, being linked to temporary capture of the soliton into the intrinsic mode of the potential well [29]. The TD effect is most pronounced at the border between the total reflection and full transmission of the soliton via RLP, as demonstrated in Fig. 6. The mechanism of the TD effect for nonlinear waves is different also from a similar effect in the linear case, where the delay is caused by multiple reflections of the wave packet inside the potential well [30]. Since linear waves do not reflect from reflectionless potentials, there is always an advance of the linear wave packet, and never a delay.

### B. Results for two-soliton molecule scattering

We begin by exploring the reflection of a soliton molecule from the modified Pöschl-Teller potential well (5). The molecule (7) with initial separation of $2x_0$ between the two solitons is set into motion with some velocity $v$ toward the potential well, situated at $x = x_p$ (see Fig. 1). The character of the scattering strongly depends on the velocity of the molecule $v$ and depth of the potential well $V_0$. For small velocities we observe total reflection as in the case of single-soliton

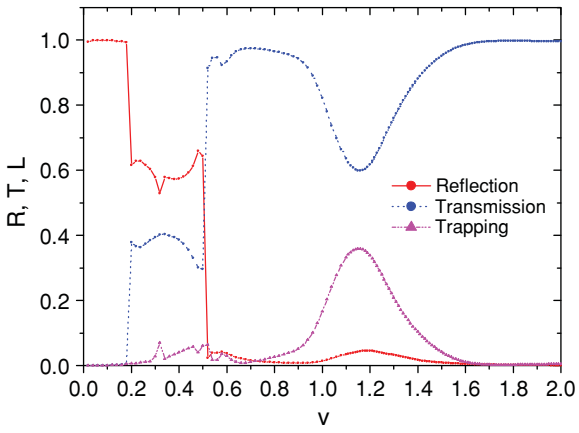


FIG. 8. (Color online) Reflected ($R$), transmitted ($T$), and trapped ($L$) part of the soliton molecule incident on the potential well (5) with parameters $V_0 = 4$, $\alpha = 2$, as a function of the incident velocity. Despite almost total reflection in the low velocity limit, and full transmission in the higher velocity limit, in most cases the soliton molecule disintegrates after the scattering event.

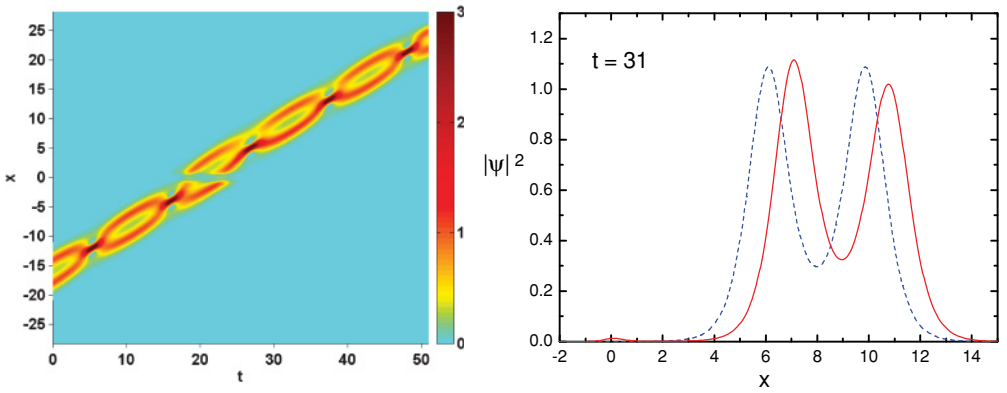


FIG. 9. (Color online) Left panel: Unscathed transmission of the soliton molecule (7) with $x_0 = 2$ incident on the potential well (5) with parameters $V_0 = 12.85$ and $\alpha = 2$. The molecule is set in motion toward the potential with the velocity $v = 0.75$, from initial position $x_p = -16$. The reflected, transmitted, and trapped parts of the wave packet, according to Eq. (6) with $b = 4$, constitute $R = 0.0017$, $T = 0.9953$, and $L = 0.003$. Right panel: Time advance of the soliton molecule's center-of-mass position resulting from this scattering event (red solid line), compared with the nonscattered counterpart (blue dashed line). Amplitudes of solitons in the molecule become slightly different after the passage of the potential well. Small structure at $x = 0$ is the trapped part of the wave packet.

scattering [1]. This is in sharp contrast to the scattering of linear wave packets, as the RLP (5) is fully transparent for linear waves of arbitrary momentum at some values of $V_0$. Specifically, the quantum mechanical transmission probability

$$T = \frac{\sinh^2(\pi v/\alpha)}{\sinh^2(\pi v/\alpha) + \cos^2\left(\frac{\pi}{2}\sqrt{1 + 8V_0/\alpha^2}\right)} \tag{24}$$

is equal to 1 for any velocity of the incident wave packet $v$, when the cosine term in the denominator vanishes at $V_0 = \alpha^2\lambda(\lambda - 1)/2$ for any integer value of $\lambda$ [9]. It does not matter what the initial shape of the wave packet may be. In contrast to this, the condition of resonant transmission ($T = 1$) through other potentials, e.g., a square well, involves both the depth of the potential and momentum of the incident wave. Consequently, only waves with wave vectors near the main wave vector of the packet are fully transmitted; other wave vectors give rise to both reflected and transmitted waves. In-depth analysis of single-soliton scattering by a square well potential has been performed in [2].

An example of the two-soliton molecule interaction with the potential (5) is illustrated in Fig. 7. We noticed periodicity of the interaction pattern when the initial position of the molecule with respect to the potential is shifted along the $x$ axis to a value $\Delta x = n\, v\, t_p$, where $n$ is an integer and $t_p$ is the period of internal oscillations of the solitons in the molecule given by Eq. (8). This suggests that the relative velocity of individual solitons in the molecule at the moment of interaction with the potential well is important for the outcome of the scattering. The key feature of this particular scattering processes is that the soliton molecule preserves its integrity after the collision. In most cases, however, the scattering process results in destruction of the molecule; i.e., individual solitons separate after the reflection, transmission, or trapping. The crucial role of the phase difference between individual solitons for the integrity of the molecule reveals itself in these scattering processes, where the phase shifts are unavoidable.

In Fig. 8 we present the reflected, transmitted, and trapped parts of the soliton molecule, calculated according to Eq. (6), as a function of the incident velocity. This figure shows that for $v < 0.18$ the molecule totally reflects from the potential well. For $0.18 < v < 0.52$ the molecule breaks into transmitted and reflected solitons. For $0.9 < v < 1.5$ we observe a more complex scattering process involving fragmentation of the molecule with significant trapping into the intrinsic mode of the potential well. For $v > 1.6$ the potential is transparent for the soliton molecule, since at such a high velocity the nonlinear term in the equation (4) is negligible compared to the kinetic energy term, and we have again the reflectionless regime, with the transmission coefficient (24) corresponding to linear case [9]. It should be noted that even in the total reflection and transmission regimes, the molecule does not necessarily maintain its molecular structure. The sharp transitions at $v = 0.18$ and $v = 0.52$ are a remarkable result of the resonant interaction between the molecule and the bound states of the potential well. A detailed account of such correlation requires further investigation. An example of nondestructive transmission of the soliton molecule through the potential well (5) is presented in Fig. 9.

## V. CONCLUSIONS

We have studied scattering of a matter-wave single soliton and two-soliton molecule incident on the attractive potential by means of the collective coordinate approach and numerical simulations of the Gross-Pitaevskii equation. Reflection is observed in a classically forbidden case, where there is no classical turning point. This kind of classically forbidden reflection, known as quantum reflection, has been demonstrated using the bound state of two solitons. The results extend the previous knowledge on single-soliton quantum reflection, reported in [1–3], to the case of composite objects like a soliton molecule. In addition, the "time advance" effect, when solitons scattered by reflectionless potentials overtake nonscattered counterparts, fully preserving their initial shape and velocity, has been studied by analytical and numerical means. A theoretical estimate of the shift of the soliton's

center of mass due to the TA effect corroborates the results of numerical simulations. The obtained results can shed new light on quantum scattering of macroscopic (many body) objects, and find application in quantum logic devices, e.g., in blocking and routing schemes for matter-waves packets. The absence of adverse effects of manipulation such as pulse deformation, emission of linear waves, and change of the soliton's velocity are among the main advantages of the proposed scheme based on RLPs.

**ACKNOWLEDGMENTS**

We acknowledge valuable discussions with J. Brand and F. Abdullaev. U.A.K. and B.B.B. thank the Department of Physics at KFUPM for its hospitality. B.B.B. is also grateful to the Saudi Center for Theoretical Physics for its material support. The remaining authors acknowledge the support of King Fahd University of Petroleum and Minerals under Project No. IN090008 and TPG101003.

[1] C. Lee and J. Brand, Europhys. Lett. **73**, 321 (2006).
[2] Th. Ernst and J. Brand, Phys. Rev. A **81**, 033614 (2010).
[3] S. L. Cornish, N. G. Parker, A. M. Martin, T. E. Judd, R. G. Scott, T. M. Fromhold, and C. S. Adams, Physica D **238**, 1299 (2009).
[4] M. Remoissenet, *Waves Called Solitons* (Springer, Berlin, 1999).
[5] S. Takagi, *Macroscopic Quantum Tunneling* (Cambridge University Press, Cambridge, 2002); M. Razavy, *Quantum Theory of Tunneling* (World Scientific, Singapore, 2003); J. Ankerhold, *Quantum Tunneling in Complex Systems* (Springer, Berlin, 2007).
[6] L. D. Carr, M. J. Holland, and B. A. Malomed, J. Phys. B **38**, 3217 (2005); Z. Duan, B. Fan, C. Yuan, J. Cheng, S. Zhu, and W. Zhang, e-print arXiv:1006.0117; L. D. Carr, R. R. Miller, and D. R. Bolton, e-print arXiv:1006.5519.
[7] G. L. Lamb Jr., *Elements of Soliton Theory* (John Wiley, New York, 1980); V. E. Zakharov, S. V. Manakov, S. P. Novikov, and L. P. Pitaevskii, *Soliton Theory. Method of Inverse Problem* (Nauka, Moscow, 1980) (in Russian; English translation: Consultants Bureau, New York, 1984).
[8] R. E. Crandall and B. R. Litt, Ann. Phys. (NY) **146**, 458 (1983); N. Kiriushcheva and S. Kuzmin, Am. J. Phys. **66**, 867 (1998).
[9] L. D. Landau and E. M. Lifschitz, *Quantum Mechanics. Nonrelativistic Theory* (Pergamon, New York, 1977); E. Merzbacher, *Quantum Mechanics* (John Wiley, New York, 1970); S. Flügge, *Practical Quantum Mechanics I* (Springer, Berlin, 1971).
[10] B. A. Malomed, in *Progress in Optics*, Vol. 43, edited by E. Wolf (Elsevier, Amsterdam, 2002), p. 69.
[11] Y. S. Kivshar, F. Zhang, and L. Vázquez, Phys. Rev. Lett. **67**, 1177 (1991); F. Zhang, Y. S. Kivshar, B. A. Malomed, and L. Vázquez, Phys. Lett. A **159**, 318 (1991).
[12] F. Zhang, Y. S. Kivshar, and L. Vázquez, J. Phys. Soc. Jpn. **63**, 466 (1994); Y. S. Kivshar, D. E. Pelinovsky, T. Cretegny, and M. Peyrard, Phys. Rev. Lett. **80**, 5032 (1998).
[13] H. Sakaguchi and M. Tamura, J. Phys. Soc. Jpn. **73**, 503 (2004).
[14] M. Stratmann, T. Pagel, and F. Mitschke, Phys. Rev. Lett. **95**, 143902 (2005); A. Hause, H. Hartwig, B. Seifert, H. Stolz, M. Bohm, and F. Mitschke, Phys. Rev. A **75**, 063836 (2007); A. Hause, H. Hartwig, M. Bohm, and F. Mitschke, *ibid.* **78**, 063817 (2008).
[15] U. Al Khawaja, Phys. Rev. E **81**, 056603 (2010).
[16] E. Tiesinga, B. J. Verhaar, and H. T. C. Stoof, Phys. Rev. A **47**, 4114 (1993); E. Timmermans, P. Tommasini, M. Hussein, and A. Kerman, Phys. Rep. **315**, 199 (1999); T. Kohler, K. Goral, and P. S. Julienne, Rev. Mod. Phys. **78**, 1311 (2006); C. Chin, R. Grimm, P. Julienne, and E. Tiesinga, *ibid.* **82**, 1225 (2010).
[17] K. E. Strecker, G. B. Partridge, A. G. Truscott, and R. G. Hulet, Nature (London) **417**, 150 (2002); L. Khaykovich, F. Schreck, G. Ferrari, T. Bourdel, J. Cubizolles, L. D. Carr, Y. Castin, and C. Salomon, Science **296**, 1290 (2002).
[18] F. Kh. Abdullaev, A. Gammal, A. M. Kamchatnov, and L. Tomio, Int. J. Mod. Phys. B **19**, 3415 (2005); R. Carretero-Gonzalez, D. J. Frantzeskakis, and P. G. Kevrekidis, Nonlinearity **21**, R139 (2008).
[19] A. Hasegawa and Y. Kodama, *Solitons in Optical Communications* (Oxford University Press, Oxford, 1995).
[20] U. Al Khawaja, H. T. C. Stoof, R. G. Hulet, K. E. Strecker, and G. B. Partridge, Phys. Rev. Lett. **89**, 200404 (2002); V. P. Barros, M. Brtka, A. Gammal, and F. Kh. Abdullaev, J. Phys. B **38**, 4111 (2005); V. S. Gerdjikov, B. B. Baizakov, M. Salerno, and N. A. Kostov, Phys. Rev. E **73**, 046606 (2006); N. G. Parker, S. L. Cornish, C. S. Adams, and A. M. Martin, J. Phys. B **40**, 3127 (2007); A. D. Martin, C. S. Adams, and S. A. Gardiner, Phys. Rev. Lett. **98**, 020402 (2007).
[21] H. Friedrich and J. Trost, Phys. Rep. **397**, 359 (2004).
[22] J. P. Gordon, Opt. Lett. **8**, 596 (1983).
[23] D. Anderson and M. Lisak, Opt. Lett. **11**, 174 (1986).
[24] Y. Kodama and K. Nozaki, Opt. Lett. **12**, 1038 (1987).
[25] G. A. Korn and T. M. Korn, *Mathematical Handbook for Scientists and Engineers: Definitions, Theorems and Formulas for Reference and Review* (McGraw-Hill, New York, 1961).
[26] G. P. Agrawal, *Nonlinear Fiber Optics* (Academic Press, New York, 1995).
[27] P. Berg, F. If, P. L. Christiansen, and O. Skovgaard, Phys. Rev. A **35**, 4167 (1987).
[28] W. H. Press, S. A. Teukolsky, W. T. Vetterling, and B. P. Flennary, *Numerical Recipes. The Art of Scientific Computing* (Cambridge University Press, Cambridge, 1996).
[29] R. H. Goodman, P. J. Holmes, and M. I. Weinstein, Physica D **192**, 215 (2004).
[30] D. Bohm, *Quantum Theory* (Prentice-Hall, New York, 1952).